Modeling and Control of an Integrated Wind Power Generation and Energy Storage System

Zhenhua Jiang, *Senior Member, IEEE*, and Xunwei Yu

Abstract – **Wind energy is gaining the most interest among a variety of renewable energy resources, but the disadvantage is that wind power generation is intermittent, depending on weather conditions. Energy storage is necessary to get a smooth output from a wind turbine. This paper presents a new integrated power generation and energy storage system for doubly-fed induction generator based wind turbine systems. A battery energy storage system is connected to the DC link of the back-to-back power converters of the doubly-fed induction generator through a bi-directional DC/DC power converter. The energy storage device is controlled so as to smooth out the total output power as the wind speed varies. Control algorithms are developed for the grid-side converter, rotor-side converter and battery converter, and are tested on a simulation model developed in MATLAB/Simulink. The model contains a DFIG wind turbine, three PWM power converters and associated controllers, a DC-link capacitor, a battery, and an equivalent power grid. Simulation studies are carried out on a 2MW DFIG wind turbine and the results suggest that the integrated power generation and energy storage system can supply steady output power as the wind speed changes.**

Index Terms—**Integrated energy system, wind turbine, doubly fed induction generator, energy storage, power converters, battery**

I. Introduction

RENEWABLE energy is increasingly attractive in solving global problems such as the environmental pollution and energy shortage. Among a variety of renewable energy resources, wind power is drawing the most attention from the government, academia, utilities and industry [1]-[9]. However, the disadvantage is that wind power generation is intermittent, depending upon weather conditions. Short-term energy storage is necessary in order to get a smooth power output from a wind turbine [10]-[13].

Compared with the wind turbines based on synchronous generators, the doubly-fed induction generator (DFIG) based wind generation technology has several advantages such as flexible active and reactive power control capabilities, lower converter costs and lower power losses [14]-[17]. In the DFIG concept, the induction generator is directly connected to the grid at the stator terminals, but the rotor terminals are connected to the grid via a variable-frequency AC/DC/AC converter. When the wind speed varies, controlling two back-to-back four-quadrant power converters connected between the rotor side and the grid side can make the rotor flux rotate from a subsynchronous speed to a supersynchronous speed. The DFIG can produce and inject constant-frequency power to the grid by controlling the rotor flux. The power converter only needs to handle a fraction (typically 25-30%) of the total power to achieve full control of the generator.

To address the intermittency problem, this paper presents an integrated power generation and energy storage system for doubly-fed induction generator based wind turbine systems. A battery energy storage system is connected to the DC link of the back-to-back power converters of the doubly-fed induction generator through a bi-directional DC/DC power converter. With this configuration, the power converters could be rated at lower power levels, compared with traditional configuration where the battery is directly tied to the DC link of the rectifier-inverter pair connected to the generator terminal. The energy storage device is controlled so as to smooth out the total output power from the wind turbine as the wind speed varies. Control algorithms are developed for the grid-side converter, rotor-side converter and battery converter, and the control strategies are tested on a simulation model developed in MATLAB/Simulink. The model contains a DFIG wind turbine, three power converters and associated controllers, a DC-link capacitor, a battery, and an equivalent power grid. In the following, a detailed time-average model for the integrated system is derived in Section II. Section III presents the control schemes for the three power converters. Simulation studies are carried out and the results are presented in Section IV. The results suggest that the integrated power generation and energy storage system can supply steady power to the grid as the wind speed varies and that the proposed control algorithms work very well under changing operating conditions.

II. Integrated Wind Power Generation and Energy Storage System

Fig. 1 schematically shows the proposed integrated power generation and energy storage system for wind-turbine systems. The wind turbine is mechanically connected to the doubly-fed induction generator through a gearbox and a coupling shaft system. The wound-rotor induction generator is fed from both the stator and rotor sides. The stator is directly connected to the grid while the rotor is fed through two back-to-back four-quadrant PWM power converters (a rotor-side converter and a grid-side converter) connected by a DC-link capacitor. The power flows from/to the rotor and the stator can be controlled both in magnitude and in direction so that it is possible to generate electrical power at constant voltage and

This work was supported in part by the National Science Foundation under grants ECCS-0652300, ECCS-0748032 and ECCS-0821126.

Z. Jiang and X. Yu are with the Department of Electrical and Computer Engineering, University of Miami, Coral Gables, FL 33146, USA (e-mail: zjiang1@miami.edu).

978-1-4244-4241-6/09/$25.00 ©2009 IEEE

constant frequency at the stator terminal and inject it into the grid over a wide operating range. A battery energy storage system is connected to the DC-link capacitor through a bi-directional DC/DC power converter. During transient disturbances or faults, a crow-bar circuit, which is not shown in the figure for simplicity of circuit diagram, can be activated to dump excess power from the rotor by short-circuiting the rotor-side converter in order to protect it from over-current in the rotor circuit.

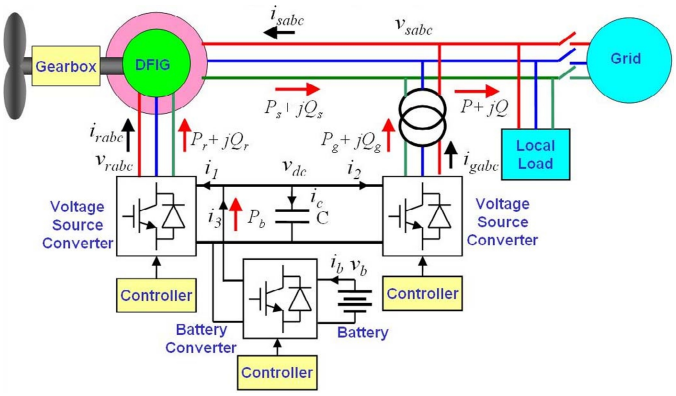

Fig. 1. Illustration of an integrated wind power generation and energy storage system connected to a utility grid.

The integrated wind power generation and energy storage system is regulated by a control system, which consists of two parts: the electrical control of the DFIG and the mechanical control of the wind turbine blade pitch angle. This paper focuses on the control of the electrical power flow, which is achieved by control of three power converters, i.e., control of the rotor-side converter, control of the stator-side converter, and control of the battery converter, as shown in Fig. 1.

A. Modeling of the Induction Generator

The induction generator considered in this study is a wound rotor induction machine fed by two back-to-back converters. In terms of the instantaneous variables shown in Fig. 1, the stator and rotor voltage equations in the stationary frame can be written in matrix form as follows [18]-[19].

$$v_{sabc} = R_s i_{sabc} + \frac{d\lambda_{sabc}}{dt} \tag{1}$$

$$v_{rabc} = R_r i_{rabc} + \frac{d\lambda_{rabc}}{dt} \tag{2}$$

Transforming to a synchronously rotating d-q reference frame [18]-[19], the voltage equations (1) and (2) become

$$v_{sd} = R_s i_{sd} - \omega_s \lambda_{sq} + \frac{d\lambda_{sd}}{dt} \tag{3}$$

$$v_{sq} = R_s i_{sq} + \omega_s \lambda_{sd} + \frac{d\lambda_{sq}}{dt} \tag{4}$$

$$v_{rd} = R_r i_{rd} - (\omega_s - \omega_r)\lambda_{rq} + \frac{d\lambda_{rd}}{dt} \tag{5}$$

$$v_{rq} = R_r i_{rq} + (\omega_s - \omega_r)\lambda_{rd} + \frac{d\lambda_{rq}}{dt} \tag{6}$$

where ω_s is the rotational angular speed of the synchronous d-q reference frame, ω_r is the rotational angular speed of the rotor, and the stator and rotor flux linkages are given by

$$\lambda_{sd} = L_{ls} i_{sd} + L_m (i_{sd} + i_{rd}) = L_s i_{sd} + L_m i_{rd} \tag{7}$$

$$\lambda_{sq} = L_{ls} i_{sq} + L_m (i_{sq} + i_{rq}) = L_s i_{sq} + L_m i_{rq} \tag{8}$$

$$\lambda_{rd} = L_{lr} i_{rd} + L_m (i_{sd} + i_{rd}) = L_m i_{sd} + L_r i_{rd} \tag{9}$$

$$\lambda_{rq} = L_{lr} i_{rq} + L_m (i_{sq} + i_{rq}) = L_m i_{sq} + L_r i_{rq} \tag{10}$$

where $L_s = L_{ls} + L_m$, $L_r = L_{lr} + L_m$ are the stator and rotor inductances, L_{ls}, L_{lr} and L_m are the stator leakage, rotor leakage and mutual inductances, respectively. The electromagnetic torque produced by the generator can be expressed as

$$T_e = n_p \left(\lambda_{sq} i_{sd} - \lambda_{sd} i_{sq}\right) = n_p L_m \left(i_{sd} i_{rq} - i_{sq} i_{rd}\right) \tag{11}$$

where n_p is the number of pole pairs.

Ignoring the power losses in the stator and rotor resistances, the active and reactive powers from the stator are given by

$$P_s = -1.5 \cdot \left(v_{sd} i_{sd} + v_{sq} i_{sq}\right) \tag{12}$$

$$Q_s = -1.5 \left(v_{sq} i_{sd} - v_{sd} i_{sq}\right) \tag{13}$$

and the active and reactive rotor powers into the rotor are

$$P_r = 1.5 \cdot \left(v_{rd} i_{rd} + v_{rq} i_{rq}\right) \tag{14}$$

$$Q_r = 1.5 \cdot \left(v_{rq} i_{rd} - v_{rd} i_{rq}\right) \tag{15}$$

The electromechanical dynamic equation is given by

$$n_p J \frac{d\omega_m}{dt} = T_m - T_e - D_m \omega_m \tag{16}$$

where T_m is the mechanical torque provided to the machine, the electromagnetic torque T_e is in the opposite direction of mechanical torque, ω_m is the rotational angular speed of the lumped-mass shaft system and $\omega_m = n_p \omega_r$, D_m is the damping of the shaft system. Since the rotor magneto-motive force has to be in synchronism with the stator magneto-motive force, the frequency of the rotor current, or the slip frequency, ω_{slip}, is

$$\omega_{slip} = \omega_s - \omega_r = s\omega_s \tag{17}$$

B. Modeling of Power Converters

Time-average models are developed for two back-to-back voltage source converters in the rotating d-q frames and for the DC/DC power converter in the stationary frame.

1) Rotor-Side Converter

The rotor-side converter is a four-quadrant PWM converter connected to the rotor terminals through three filter inductors. The voltage equations in the d-q frame rotating at the angular frequency of ω_1 are as follows.

$$v_{rd} = d_{d1} v_{dc} + \omega_1 L_1 i_{rq} - L_1 \frac{di_{rd}}{dt} \tag{18}$$

$$v_{rq} = d_{q1} v_{dc} - \omega_1 L_1 i_{rd} - L_1 \frac{di_{rq}}{dt} \tag{19}$$

where $\omega_1 = \omega_s - \omega_r$ is the angular frequency of the rotor currents. The rotor-side converter can be represented by a current-controlled voltage source, as shown in Fig. 2.

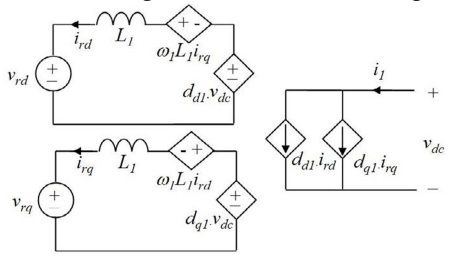

Fig. 2. Time-average model of the rotor-side converter.

2) Stator-Side Converter

The stator-side converter is a four-quadrant PWM converter connected to the stator terminals through three filter inductors. The voltage equations in the *d-q* frame rotating at the angular frequency of ω_2 are as follows.

$$v_{gd} = d_{d2} v_{dc} + \omega_2 L_2 i_{gq} - L_2 \frac{di_{gd}}{dt} \tag{20}$$

$$v_{gq} = d_{q2} v_{dc} - \omega_2 L_2 i_{gd} - L_2 \frac{di_{gq}}{dt} \tag{21}$$

where $\omega_2 = \omega_s$ is the angular frequency of the stator voltages. The rotor-side converter is represented by a current-controlled voltage source, as shown in Fig. 3.

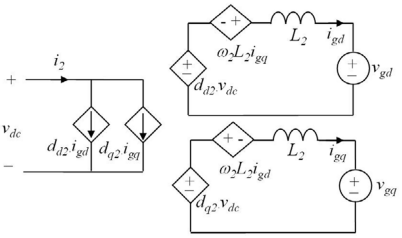

Fig. 3. Time-average model of the stator-side converter.

3) Battery Converter

The battery converter is used to support the DC-link voltage. The rotor-side converter draws the current $i_1 = d_{d1} i_{rd} + d_{q1} i_{rq}$ from the DC-link, while the stator-side converter draws $i_2 = d_{d2} i_{gd} + d_{q2} i_{gq}$ from the DC-link. Neglecting the switching and conduction losses in these converters and the power losses in the dc-link, the battery converter and the DC-link dynamics are governed by

$$v_b = L_b \frac{di_b}{dt} + (1 - d_b) v_{dc} \tag{22}$$

$$i_c = i_3 - i_1 - i_2 = (1 - d_b) i_b - i_1 - i_2 = C \frac{d v_{dc}}{dt} \tag{23}$$

The battery converter is represented by a voltage-controlled current source, as shown in Fig. 4. At steady state, $P_b = P_r + P_g$ and $i_3 = i_1 + i_2$; thus the DC-link voltage, v_{dc}, stays constant with negligible ripples. However, when a disturbance occurs, the relationship, $P_b = P_r + P_g$, is broken and the current flowing through the DC-link capacitor, $i_c = i_3 - i_1 - i_2$, is not zero, which results in fluctuations of the DC-link voltage v_{dc}. The battery provides or absorbs an appropriate amount of current to support the DC-link voltage.

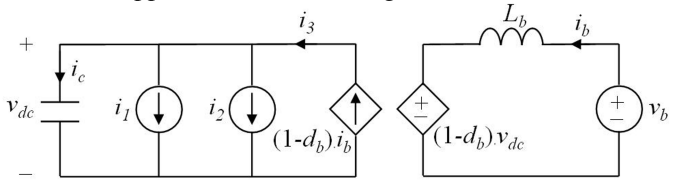

Fig. 4. Time-average model of the battery converter.

C. Modeling of Battery Energy Storage System

The battery is modeled as a nonlinear voltage source whose output voltage depends not only on the current but also on the battery state of charge, SOC, which is a nonlinear function of the current and time, as given by

$$v_b = V_0 - R_b \cdot i_b - K \frac{Q}{Q - \int i_b dt} + A \cdot \exp(-B \int i_b dt) \tag{24}$$

$$SOC = 100 \left(1 - \frac{\int i_b dt}{Q} \right) \tag{25}$$

where, R_b is the internal resistance of the battery, V_0 the open-circuit potential (V), K the polarization voltage (V), Q the battery capacity (Ah), A the exponential voltage (V), and B the exponential capacity (Ah).

III. Control of Power Converters

The objective of the rotor-side converter is to manage the active power and reactive power from the stator terminals independently; while the objective of the stator-side converter is to manage the active power and reactive power from the stator-side converter independently. The battery converter is to keep the DC-link voltage constant regardless of the magnitude and direction of the rotor and stator powers. The goal of these three converters is to maintain a constant total power output from the wind turbine generator. The design procedure of the control system is discussed below.

A. Control of Rotor-Side Converter

The rotor-side converter control scheme consists of two cascaded control loops. The inner current control loops regulate independently the *d*-axis and *q*-axis rotor current components, i_{dr} and i_{qr}, according to a synchronously rotating reference frame where the voltage oriented vector control is used. The outer control loops regulate the active power and reactive power output from the machine stator independently.

In the stator voltage oriented reference frame, the *d*-axis is aligned with the stator voltage vector, namely, $\boldsymbol{v_s}$. The stator flux linkage vector $\boldsymbol{\lambda_s}$ is then aligned with the *q*-axis, i.e., $\lambda_{sq} = \lambda_s = L_m i_{ms}$ and $\lambda_{sd} = 0$. Considering (3)-(10), we can get the following relationships.

$$i_{sd} = -L_m i_{rd} / L_s \tag{26}$$

$$i_{sq} = L_m (i_{ms} - i_{rq}) / L_s \tag{27}$$

$$P_s = 1.5 \cdot \omega_s L_m^2 i_{ms} i_{rd} / L_s \tag{28}$$

$$Q_s = 1.5 \cdot \omega_s L_m^2 i_{ms} (i_{rq} - i_{ms}) / L_s \tag{29}$$

$$v_{rd} = R_r i_{rd} + \sigma L_r \frac{di_{rd}}{dt} - (\omega_s - \omega_r)(\sigma L_r i_{rq} + L_m^2 i_{ms} / L_s) \tag{30}$$

$$v_{rq} = R_r i_{rq} + \sigma L_r p i_{rq} + (\omega_s - \omega_r) L_r \frac{di_{rd}}{dt} \tag{31}$$

where i_{ms} is the exciting current and can be calculated from

$$i_{ms} = \frac{v_{sd} - r_s i_{sd}}{\omega_s L_m} \tag{32}$$

and σ is a constant

$$\sigma = \frac{L_s L_r - L_m^2}{L_s L_r} \tag{33}$$

Equations (28) and (29) indicate that with the stator voltage oriented control scheme P_s and Q_s are directly related to the *d*-axis and *q*-axis components of the rotor currents respectively and can be independently controlled by regulating the rotor

current *d*- and *q*-axis components, i_{rd} and i_{rq}, respectively. Consequently, the reference values of i_{rd} and i_{rq} can be determined from the outer power control loops.

1) Inner Current Control Loops

If the rotor windings are used as the filter of the rotor-side converter, the filter inductors shown in Fig. 2 can be omitted and the *d*-axis and *q*-axis voltages produced by the converter are proportional to the corresponding duty cycles of the pulse-width modulation signal. In (30) and (31), i_{ms} and i_{rd}, and i_{rq} are cross-coupling terms for v_{rd} and v_{rq} respectively. If these terms are regarded as disturbances and considered separately, it is possible to define

$$v_{rd}^{'} = r_r i_{rd} + \sigma L_r \frac{di_{rd}}{dt} \tag{34}$$

$$v_{rq}^{'} = r_r i_{rq} + \sigma L_r \frac{di_{rq}}{dt} \tag{35}$$

Equations (34) and (35) indicate that i_{rd} and i_{rq} independently respond to $v_{rd}^{'}$ and $v_{rq}^{'}$, respectively, and act as two linear first-order dynamic systems. If a proportional-integral (PI) control scheme is adopted to produce the references for $v_{rd}^{'}$ and $v_{rq}^{'}$ based on a current feedback control, i.e.,

$$v_{rd}^{'} = \left(k_{rdp} + \frac{k_{rdi}}{s}\right)(i_{rd}^{*} - i_{rd}) \tag{36}$$

$$v_{rq}^{'} = \left(k_{rqp} + \frac{k_{rqi}}{s}\right)(i_{rq}^{*} - i_{rq}) \tag{37}$$

then the following control laws can be derived for the rotor-side converter by substituting (36) and (37) into (30) and (31).

$$v_{rd}^{*} = \left(k_{rdp} + \frac{k_{rdi}}{s}\right)(i_{rd}^{*} - i_{rd}) - (\omega_s - \omega_r)\left(\sigma L_r i_{rq} + \frac{L_m^2}{L_s} i_{ms}\right) \tag{38}$$

$$v_{rq}^{*} = \left(k_{rqp} + \frac{k_{rqi}}{s}\right)(i_{rq}^{*} - i_{rq}) + (\omega_s - \omega_r)\sigma L_r i_{rd} \tag{39}$$

2) Active Power Control

Equation (28) suggests that the active power exchanged between the stator and the grid is proportional to i_{rd}. The following control law can be used for the rotor-side converter to regulate the active power.

$$i_{rd}^{*} = \left(k_{Psp} + \frac{k_{Psi}}{s}\right)(P_s^{*} - P_s) \tag{40}$$

3) Reactive Power Control

Equation (29) suggests that the reactive power exchanged between the stator and the grid is proportional to i_{rq}. The following control law can be used for the rotor-side converter to regulate the reactive power.

$$i_{rq}^{*} = \left(k_{Qsp} + \frac{k_{Qsi}}{s}\right)(Q_s^{*} - Q_s) \tag{41}$$

Fig. 5 shows the overall vector control scheme of the rotor-side converter. The compensated outputs of the two current controllers, v_{rd} and v_{rq}, are used by the PWM module to generate the gate control signals to drive the IGBT switches.

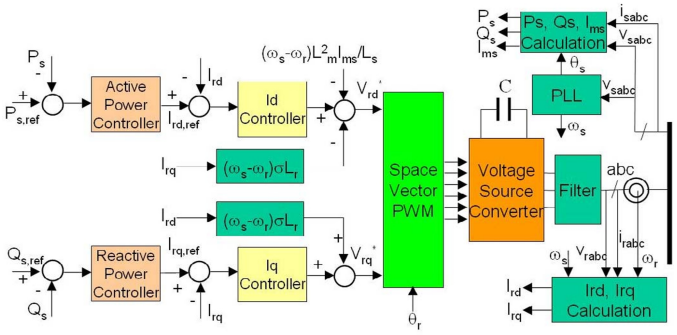

Fig. 5. Vector control scheme of the rotor-side converter ($\theta_r = \int(\omega_s - \omega_r)dt$).

B. Control of Stator-Side Converter

The stator-side converter control scheme also consists of two cascaded control loops. The inner current control loops regulate independently the *d*-axis and *q*-axis components of the stator-side converter AC output current, i_{gd} and i_{gq}, in the synchronously rotating reference frame. The outer control loops regulate the active power and reactive power exchanged between the stator-side converter and the grid.

1) Inner Current Control Loops

With the *d*-axis aligned to the grid voltage vector $\boldsymbol{v_s}$ ($v_{sd} = v_s$, $v_{sq} = 0$), the following *d-q* vector representation can be obtained for the stator-side converter

$$v_s = d_{d2} v_{dc} + \omega_s L_2 i_{gq} - L_2 \frac{di_{gd}}{dt} \tag{42}$$

$$0 = d_{q2} v_{dc} - \omega_s L_2 i_{gd} - L_2 \frac{di_{gq}}{dt} \tag{43}$$

Following the same procedure as in (34)-(39), the references for v_{gd} and v_{gq} can be obtained by the following feedback loops and PI controllers.

$$v_{gd}^{*} = \left(k_{gdp} + \frac{k_{gdi}}{s}\right)(i_{gd}^{*} - i_{gd}) - \omega_s L_2 i_{gq} + v_s \tag{44}$$

$$v_{gq}^{*} = \left(k_{gqp} + \frac{k_{gqi}}{s}\right)(i_{gq}^{*} - i_{gq}) + \omega_s L_2 i_{gd} \tag{45}$$

where i_{gd}^{*} and i_{gq}^{*} are the reference values of the converter output current obtained from the outer power control loops.

2) Active Power Control

Ignoring the power losses in the converter, the active and reactive powers from the gird-side converter are given by

$$P_g = 1.5 \cdot (v_{gd} i_{gd} + v_{gq} i_{gq}) = 1.5 \cdot v_{gd} i_{gd} \tag{46}$$

$$Q_g = 1.5 \cdot (v_{gq} i_{gd} - v_{gd} i_{gq}) = -1.5 \cdot v_{gd} i_{gq} \tag{47}$$

Since the *d*-axis voltage is maintained constant, the active power exchanged between the stator-side converter and the grid is proportional to i_{gd}. The following control law can be used for the rotor-side converter to regulate the active power.

$$i_{gd}^{*} = \left(k_{Pgp} + \frac{k_{Pgi}}{s}\right)(P_g^{*} - P_g) \tag{48}$$

3) Reactive Power Control

Equation (47) shows that the reactive power exchanged between the stator-side converter and the grid is proportional

to -i_{gq}. The following control law can be used for the stator-side converter to regulate the reactive power.

$$i_{gq}^{*} = -\left(k_{Qgp} + \frac{k_{Qgi}}{s}\right)(Q_g^{*} - Q_g) \tag{49}$$

Fig. 6 shows the overall vector control scheme of the stator-side converter. The compensated outputs of the two current controllers, v_{gd} and v_{gq}, are used by the PWM module to generate the gate control signals to drive the IGBT switches.

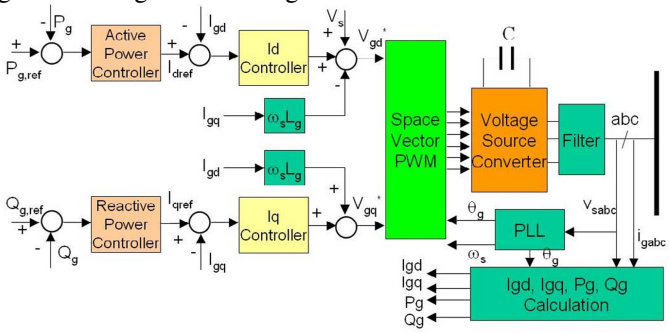

Fig. 6. Vector control scheme of the stator-side converter.

C. Control of Battery Converter

Neglecting the losses in the power converters, the battery, filtering inductors and the transformer and the harmonics due to switching actions, the power balance of the integrated wind power generation and energy storage system is governed by

$$P_b - P_r - P_g = v_{dc} i_c = C v_{dc} \frac{dv_{dc}}{dt} \tag{50}$$

The objective of the batter converter is to maintain a constant voltage at the DC link, so the ripple in the capacitor voltage is much less than the steady-state voltage. Equation (50) can be rewritten as

$$P_b - P_r - P_g \approx C V_{dc} \frac{dv_{dc}}{dt} \tag{51}$$

If the powers injected to the two back-to-back voltage source converters are assumed constant at any particular instant, the power from the battery converter is responsible to change the capacitor voltage. Therefore, the transfer function from P_g to v_{dc} is given by

$$\frac{v_{dc}(s)}{P_b(s)} = \frac{1}{C V_{dc} \cdot s} \tag{52}$$

Considering the battery voltage can be assumed constant at any instant and

$$P_b = v_b i_b = V_b i_b \tag{53}$$

equation (52) becomes

$$\frac{v_{dc}(s)}{i_b(s)} = \frac{V_b}{V_{dc}} \frac{1}{C \cdot s} \tag{54}$$

Equation (54) suggests that a linear first-order dynamics exists between the battery current and the DC link voltage. Therefore, the reference value of i_b can be generated using a voltage feedback control and a PI control scheme as follows.

$$i_b^{*} = \left(k_{vp} + \frac{k_{vi}}{s}\right)(v_{dc}^{*} - v_{dc}) \tag{55}$$

The inner current control loop is to force the battery current to follow the reference produced in (55) using a PI scheme, as given by

$$d_b = \left(k_{bp} + \frac{k_{bi}}{s}\right)(i_b^{*} - i_b) \tag{56}$$

Fig. 7 shows the overall structure of the battery converter controller.

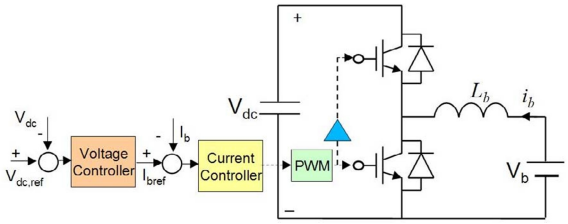

Fig. 7. Control scheme of the battery converter.

IV. Simulation Results

To verify the control strategies designed above, a single machine infinite bus (SMIB) power system, as shown in Fig. 1, is used for simulation studies in MATLAB/Simulink. A 2MW DFIG wind turbine system is connected to the stiff grid through a step-up transformer and transmission lines. The proposed integrated power generation and energy storage configuration is used. The parameters of the DFIG wind turbine are given in the Appendix. Two scenarios are studied where the output power to the grid and the wind speed are changed.

A. Case I: Change in Output Power to Grid

The wind turbine operates at a constant speed with the DFIG's input mechanical power P_m = 2MW. The reference output power from the generator stator is set as $P_{s,ref}$ = 1.8MW and $Q_{s,ref}$ = 0, respectively. The reference output power from the stator-side converter is initially set as $P_{g,ref}$ = 0.24MW and $Q_{g,ref}$ = 0.1Mvar. The reference active power is changed to 0.3MW at 1s and to 0.2MW at 3s, while the reference reactive power is changed to 0.2Mvar at 5s. This case can simulate the operation condition where there is a change in the load while the power from the stator terminals is maintained constant. This operation condition is good for the shaft due to a constant electromagnetic torque. The simulation results are shown in Fig. 8.

As shown in Fig. 8-a, the DFIG's input mechanical power and the stator's output power are kept constant; according to the control method discussed before, the DFIG's rotor current is constant correspondingly, as shown in Fig. 8-c. The battery initially discharges a small amount of power, as shown in Fig. 8-a, at a low current (Fig. 8-d) through the rotor-side converter to meet the difference between the stator output power and the input mechanical power. As the stator-side converter increases its output power, the battery discharges more power to balance the increased power difference. However, when the output power from the stator-side converter decreases to 0.2MW, the battery starts to be charged (Fig. 8-d) and a certain amount of power is delivered to the battery. The power of the stator-side converter is controlled by its *d*-axis current, as shown in Fig. 8-c, which agrees with (47). The change in the output reactive power (Fig. 8-b) doesn't affect the battery current (Fig. 8-d), but the *q*-axis current of the stator-side converter (Fig. 8-c).

Fig. 8-d shows that the voltage across the DC-link capacitor undergoes very slight disturbances as the battery current changes, which suggests that the battery can help stabilize the DC-link voltage.

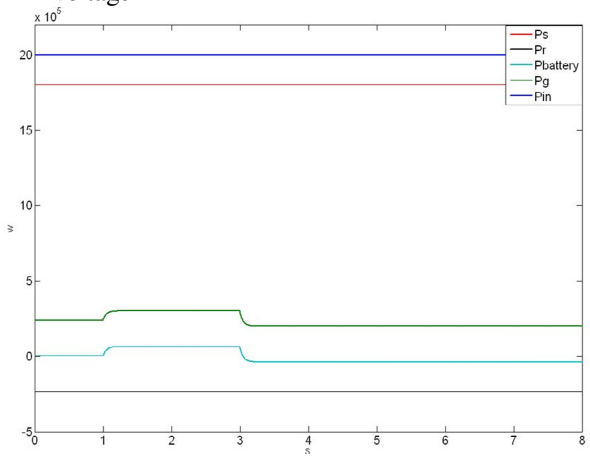

(a) Input mechanical power, DFIG stator output power, rotor power, battery power and stator-side converter output power

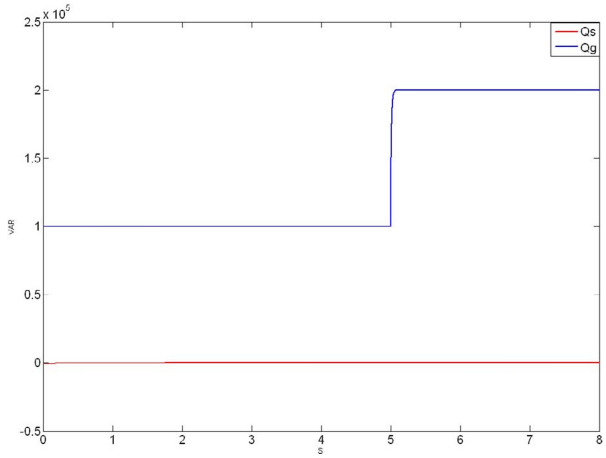

(b) DFIG stator output reactive power and stator-side converter output reactive power

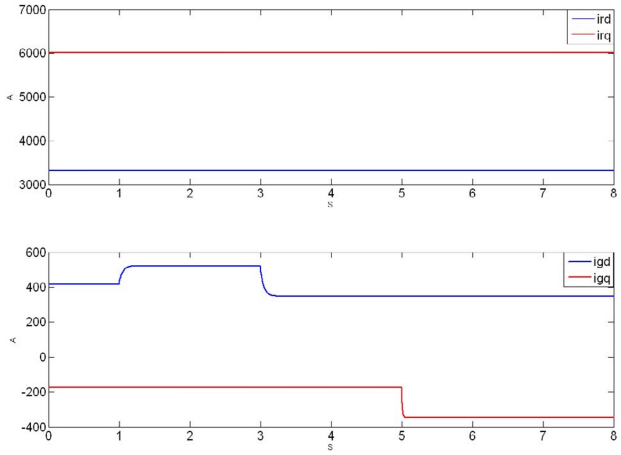

(c) Rotor currents i_{rd} and i_{rq}, and stator-side converter currents i_{gd} and i_{gq}

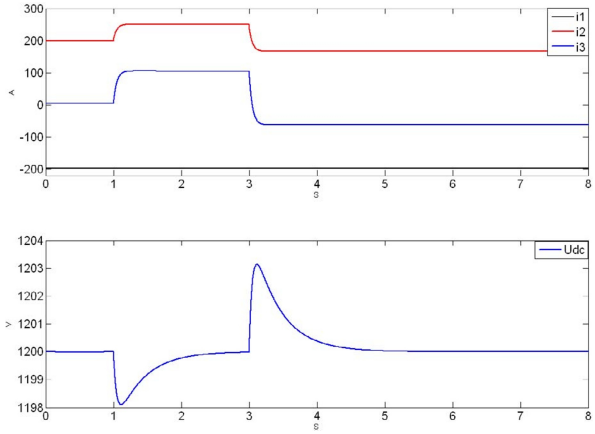

(d) Currents i_1, i_2 and i_3, and DC-link voltage U_{dc}

Fig. 8. Simulation results in the case where the output power to the grid is changed.

B. Case II: Change in Wind Speed

In this case, the wind turbine operates at varying speeds, which means the input mechanical power to the DFIG is changing. In the simulation, the input mechanical power is initially set to P_m = 2MW and then changed to 1.7MW at 1s, to 2.3MW at 3s, and back to 2MW at 5s. The reference output power from the generator stator terminals is set as $P_{s,ref}$ = 1.8MW and $Q_{s,ref}$ = 0, respectively. The reference output power from the stator-side converter is set as $P_{g,ref}$ = 0.24MW and $Q_{g,ref}$ = 0.1MVar. The simulation results are shown in Fig. 9.

Initially the battery discharges a very low current through the rotor-side converter (Fig. 9-d) because the DFIG's input mechanical power is slightly less than the total output power (i.e., the stator output power plus the stator-side converter output power), as shown in Fig. 9-a. As the input mechanical power decreases to 1.7MW, the battery discharges more power to balance the increased power difference. However, when the input mechanical power increases to 2.4MW, the battery starts to be charged (Fig. 9-d) and a certain amount of power is delivered to the battery. The rotor-side converter outputs power from the rotor. The active power of the rotor-side converter is controlled by its *d*-axis current, as shown in Fig. 9-c, which agrees with (28). The change in the input mechanical power affects the reactive power slightly as shown in Fig. 9-b, which is reflected in the change in *q*-axis current (Fig. 9-c). As the input mechanical power is changed back to 2MW, the battery starts to discharge again. Fig. 9-d shows that the voltage across the DC-link capacitor undergoes slight disturbances as the battery current changes, which suggests that the battery can help stabilize the DC-link voltage.

Because the input wind power changes and the stator output power is kept constant, the DFIG switches between the subsynchronous mode and the supersynchronous mode during the operation period, which can be seen from Fig. 9-e. When the DFIG operates in the subsynchronous mode, the generator rotor accepts active power from the DC link and the required power will be supplied by the battery, which means that the rotor-side converter operates in the inverter mode. On the other hand, as the DFIG works in the supersynchronous mode,

active power will be delivered from the rotor to the DC link. In this mode, whether the battery is charged or discharged will depend on the difference between the rotor output power and the grid-side converter output power. If the rotor output power is larger than the grid-side converter output power, the battery will accept the remaining power. While the rotor output power is less than the grid-side converter output power, the battery will export the rest of the power. Since the DC-link voltage is controlled by the battery converter, the output power of the stator-side converter will not depend on the rotor-side output power. That explains why the stator-side converter output power is not affected by the rotor-side power variations.

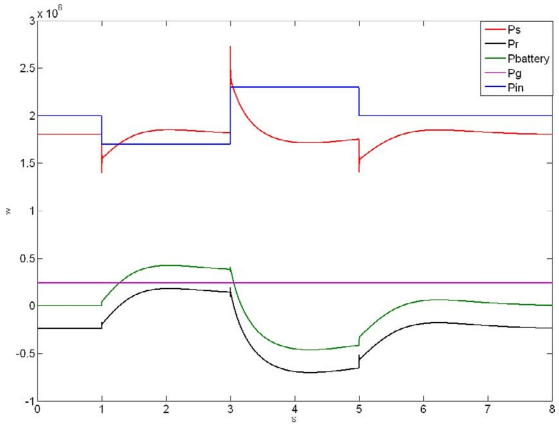

(a) Input mechanical power, DFIG stator output power, rotor power, battery power and stator-side converter output power

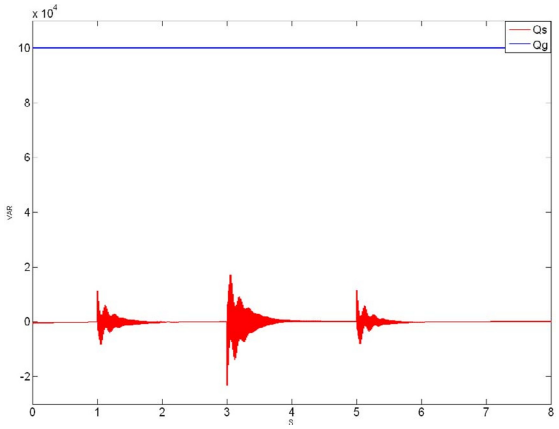

(b) DFIG stator output reactive power and stator-side converter output reactive power

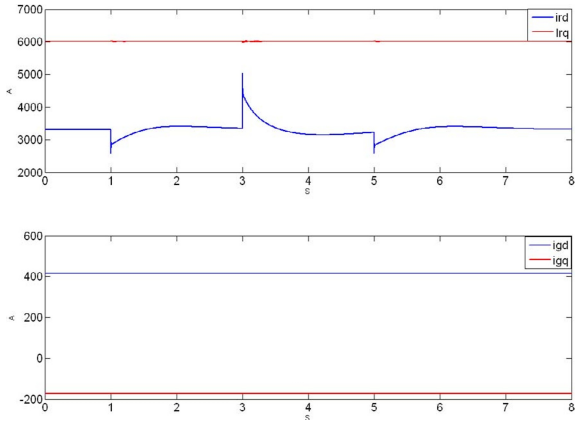

(c) Rotor currents i_{rd} and i_{rq}, and stator-side converter currents i_{gd} and i_{gq}

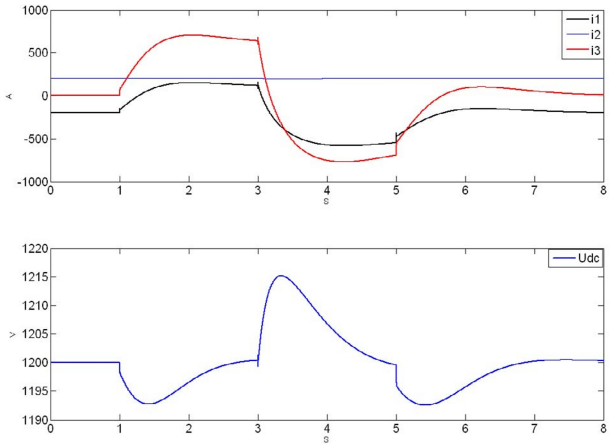

(d) Currents i_1, i_2 and i_3, and DC-link voltage U_{dc}

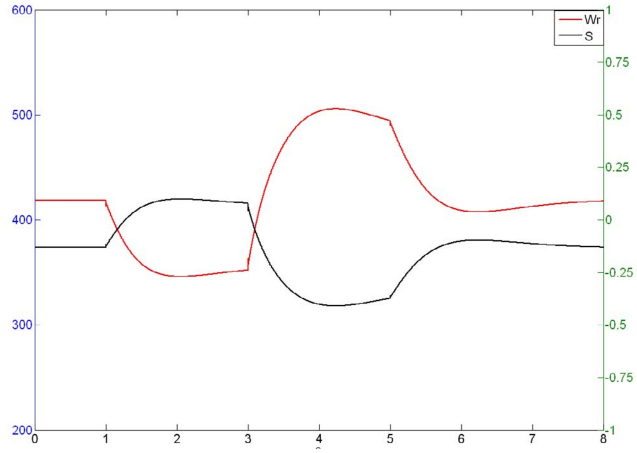

(e) Rotor speed and the slip

Fig. 9. Simulation results in the case where the wind speed is changed.

V. Conclusion

An integrated power generation and energy storage system has been presented for doubly-fed induction generator based wind turbine systems. A battery energy storage system is connected to the DC link of the back-to-back power converters of the doubly-fed induction generator through a bi-directional DC/DC power converter. The battery is charged if there is excess power and can supply power to the load if the power demand is higher than the input mechanical power form the wind. The energy storage device is controlled so as to smooth out the output power as the wind speed varies or maintain a desirable power output. Control algorithms are developed for the grid-side converter, rotor-side converter and battery converter, and the control strategies are tested on a simulation model of a 2MW DFIG wind turbine system developed in MATLAB/Simulink. The model contains a DFIG wind turbine, three power converters build with individual IGBT switches, a DC-link capacitor, and several controllers. Simulation results show that the integrated power generation and energy storage system can supply steady output power as the wind speed changes. As the wind speed is constant, the wind turbine can output varying power due to the existence of the battery. This study suggests that the integrated power generation and energy storage system is good for intermittent wind power generation.

APPENDIX

Table I. System parameters used in the simulation

Parameters	Values (p.u.)	Parameters	Values
L_{ls}	0.171	V_{dc_nom}	1200 (V)
L_{lr}	0.156	C	0.06 (F)
L_m	2.9	V_{nom}	575 (V)
R_s	0.0071	P_{nom}	10 (MW)
R_r	0.005	$V_{battery}$	600 (V)
		n_p	6

REFERENCES

[1] M. V. A. Nunes, J. A. Pecas Lopes, H. H. Zurn, U. H. Bezerra, and R. G. Almeida, "Influence of the variable-speed wind generators in transient stability margin of the conventional generators integrated in electrical grids," *IEEE Trans. Energy Conversion*, vol. 19, no. 4, pp. 692-701, Dec. 2004.

[2] H. Akagi, H.Sato, "Control and performance of a doubly-fed induction machine intended for a flywheel energy storage system," *IEEE Trans. Power Electron*, vol. 17, no. 1, pp. 109-116, Jan. 2002.

[3] F. M Hughes, O. Lara, N. Jenkins, and G. Strbac, "A power system stabilizer for DFIG-based wind generation," *IEEE Transactions on Power Systems*, Vol. 21, No. 2, pp. 763 – 772, May. 2006.

[4] Y. Lei, A. Mullane, G. Lightbody, and R. Yacamini, "Modeling of the wind turbine with a doubly fed induction generator for grid integration studies," *IEEE Trans. Energy Conversion*, vol. 21, no. 1, pp. 257-264, Mar. 2006.

[5] V. Akhmatov, "Analysis of Dynamic Behavior of Electric Power Systems with Large Amount of Wind Power," Ph.D. dissertation, Technical University of Denmark, Kgs. Lyngby, Denmark, Apr. 2003.

[6] J. Morren and S. W. H. de Haan, "Ridethrough of wind turbines with doubly-fed induction generator during voltage dip," *IEEE Trans. Energy Conversion*, vol. 20, no. 2, pp. 435-441, Jun. 2005.

[7] T. Petru and T. Thiringer, "Modeling of wind turbines for power system studies," *IEEE. Trans. Power Systems*, vol. 17, no. 4, Nov. 2002, pp. 144-151.

[8] J. G. Slootweg, S. W. H. de Hann, H. Polinder, and W. L. Kling, "General model for representing variable speed wind turbines in power system dynamic simulations," *IEEE. Trans. Power Systems*, vol. 18, no. 1, pp. 1132-1139, Feb. 2003.

[9] L. Xu, P. Cartwright, "Direct active and reactive power control of DFIG for wind energy generation," *IEEE Transactions on Energy Conversion* vol. 21, Iss.3, pp.750 – 758 Sept. 2006.

[10] S. S. Choi, K. J. Tseng, D. M. Vilathgamuwa, T. D. Nguyen, "Energy storage systems in distributed generation schemes", Proceedings of 2008 IEEE Power and Energy Society General Meeting, pp. 1 – 8, 20-24 July 2008.

[11] E. Spahic, G. Balzer, A. Shakib, "The Impact of the "Wind Farm - Battery" Unit on the Power System Stability and Control", *2007 IEEE Lausanne Power Tech*, pp. 485 – 490, 1-5 July 2007.

[12] C. Abbey, K. Strunz, J. Chahwan, and G. Joos, "Impact and Control of Energy Storage Systems in Wind Power Generation", Proceedings of the 2007 Power Conversion Conference - Nagoya, pp. 1201 – 1206, 2-5 April 2007.

[13] E. Spahic, G. Balzer, B. Hellmich, W. Munch, "Wind Energy Storages – Possibilities", *2007 IEEE Lausanne Power Tech*, pp. 615 – 620, 1-5 July 2007.

[14] S. Muller, M. Dei, and R. W. Doncker, "Doubly fed induction generator systems for wind turbines," *IEEE Industry Applications Maganize*, vol. 8, Iss. 3, pp. 26 – 33, May-June 2002.

[15] S. Towito, M. Berman, G. Yehuda, and R. Rabinovici, "Distribution Generation Case Study: Electric Wind Farm with Doubly Fed Induction Generators," *IEEE 24th Convention of Electrical and Electronics Engineers in Israel*, pp. 393 – 397, Nov. 2006.

[16] S. Muller, M. Deicke, and R. W. De Doncker, "Doubly fed induction generator systems for wind turbines," *IEEE Ind. Appl , Mag,* vol. 17, no. 1, pp. 26-33, May-Jun. 2002.

[17] R. Datta and V. T. Ranganathan, "Variable-speed wind power generation using doubly fed wound rotor induction – a comparison with alternative schemes,' *IEEE Trans. Energy Conversion*, vol. 17, no. 3, pp. 414-421, Sept. 2002.

[18] D. W. Novotny and T. A. Lipo, *Vector Control and Dynamics of AC Drives*, Oxford University Press, 2000.

[19] Ned Mohan, *Advanced Electric Drives: Analysis, Control and Modeling using Simulink,* Mnpere, 2001.

BIOGRAPHIES

Zhenhua Jiang (S'01-M'03-SM'08) received the B.Sc. and M.Sc. degrees from Huazhong University of Science and Technology, Wuhan, China, in 1997 and 2000, respectively, and the Ph. D. degree from the University of South Carolina, Columbia, SC, in 2003, all in electrical engineering. He was a post-doctoral Research Fellow at the University of South Carolina, Columbia, SC, from 2003 to 2005, and an Assistant Professor in the Department of Electrical Engineering at the University of New Orleans from 2005 to 2006. He has been an Assistant Professor in the Department of Electrical and Computer Engineering at the University of Miami since 2006. His research areas include integration of distributed energy resources, microgrids, smart grid, renewable and alternative energy, energy storage, vehicular electrical power systems, multiagent based modeling and control, intelligent optimization and control, and applications of power electronics in power systems. He is a Technical Program Chair for the IEEE PES Energy Development and Power Generation Committee. He serves on the editorial board of *Simulation Modelling Practice and Theory*. He has been a reviewer for a wide range of journals including *IEEE Trans. on Energy Conversion*, *IEEE Trans. on Industry Applications*, *IEEE Trans. on Power Electronics*, *IEEE Trans. on Aerospace and Electronic Systems*, *IEEE Trans. on Industrial Electronics*, *IEEE Trans. on Automatic Control*, *IEEE Trans. on Education*, *IET Circuits, Devices & Systems, IET Electric Power Applications*, *IET Power Electronics*, *IET Generation, Transmission & Distribution*, *Simulation Modelling Practice and Theory,* and *Journal of the Franklin Institute*. He has organized or chaired several sessions and served as a Technical Program Committee member for a large number of conferences. He was a recipient of the NSF Early Faculty Career Development (CAREER) Award in 2008, and an invited participant of the U.S. National Academy of Engineering's 2008 U.S. "Frontiers of Engineering" Symposium.

Xunwei Yu received the M.Sc. degree in electrical engineering from Huazhong University of Science and Technology, Wuhan, China, in 2007. He is currently a Research Assistant in the Department of Electrical and Computer Engineering at the University of Miami, working toward his Ph.D. degree. His research interests are in control of power electronics, integration of distributed energy resources, and microgrids.